Benzenesulfonamides with different rigidity-conferring linkers as carbonic anhydrase inhibitors: an insight into the antiproliferative effect on glioblastoma, pancreatic, and breast cancer cells

Francesco Liguori, Simone Carradori, Roberto Ronca, Sara Rezzola, Serena Filiberti, Fabrizio Carta, Marta Turati & Claudiu T. Supuran

Taylor & Francis
Taylor & Francis Group

SHORT COMMUNICATION

🔓 OPEN ACCESS ✓ Check for updates

Benzenesulfonamides with different rigidity-conferring linkers as carbonic anhydrase inhibitors: an insight into the antiproliferative effect on glioblastoma, pancreatic, and breast cancer cells

Francesco Liguori[a,b], Simone Carradori[a] 🆔, Roberto Ronca[c], Sara Rezzola[c], Serena Filiberti[c], Fabrizio Carta[b], Marta Turati[c] and Claudiu T. Supuran[b] 🆔

[a]Department of Pharmacy, "G. d'Annunzio" University of Chieti-Pescara, Chieti, Italy; [b]Neurofarba Department, University of Florence, Florence, Italy; [c]Department of Molecular and Translational Medicine, University of Brescia, Brescia, Italy

ABSTRACT

Among the chemotypes studied for selective inhibition of tumour-associated carbonic anhydrases (CAs), **SLC-0111**, a ureido-bearing benzenesulfonamide CA IX inhibitor, displayed promising antiproliferative effects in cancer cells *in vitro* and *in vivo*, being in Phase Ib/II clinical development. To explore the structural characteristics required for better discrimination of less conserved regions of the enzyme, we investigate the incorporation of the urea linker into an imidazolidin-2-one cycle, a modification already explored previously for obtaining CA inhibitors. This new library of compounds inhibited potently four different hCAs in the nanomolar range with a different isoform selectivity profile compared to the lead **SLC-0111**. Several representative CA IX inhibitors were tested for their efficacy to inhibit the proliferation of glioblastoma, pancreatic, and breast cancer cells expressing CA IX, in hypoxic conditions. Unlike previous literature data on **SLC-149**, a structurally related sulphonamide to compounds investigated here, our data reveal that these derivatives possess promising anti-proliferative effects, comparable to those of **SLC-0111**.

GRAPHICAL ABSTRACT
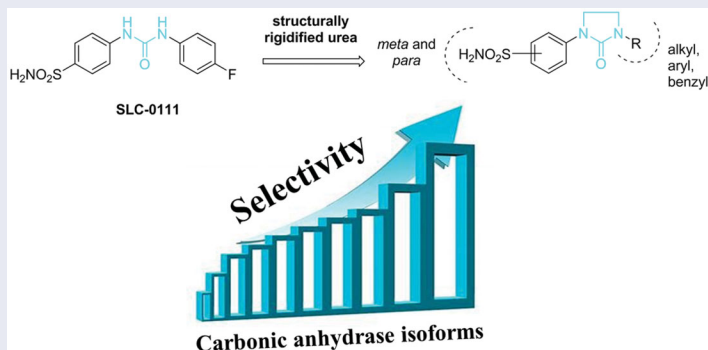
1. Introduction

Carbonic anhydrases (CAs, E.C. 4.2.1.1) are among the most studied metalloenzymes in Medicinal Chemistry. They are grouped into eight gene families and are present both in eukaryotes and prokaryotes[1]. In such organisms, they catalyse the carbon dioxide (CO_2) interconversion into bicarbonate (HCO_3^-) and proton (H^+) useful to physiologically/pathologically modulate pivotal cell processes, such as transport of CO_2/HCO_3^- between lungs and metabolising tissues, electrolyte secretion in tissues/organs using CO_2 and pH homeostasis, bone remodelling, metabolic reactions (lipogenesis, gluconeogenesis, and ureagenesis), and tumorigenicity, at least in vertebrates[1,2]. The large plethora of therapeutic

applications, e.g. epilepsy, glaucoma, idiopathic intracranial hypertension, and altitude sickness, with many inhibitors in the clinical use, allowed the wide exploration of CA modulators (inhibitors and activators) through the design of novel chemical scaffolds/chemotypes[3,4]. Accumulating evidence over the last two decades demonstrated the crucial role of the membrane-bound CA IX and XII (also called tumour-associated CAs) in the maintenance of a favourable intra-/extra-cellular pH for tumour cell survival and growth. Their hypoxia-inducible factors 1α (HIF-1α)-mediated overexpression as well as tissue/cell localisation pinpointed that these isozymes are responsible for cancer cell migration, invasion, and maintenance of stemness through the development of chemoresistance and in malignant progression[5–7]. Indeed, they can be

Figure 1. Previously described benzenesulfonamide ureas and rational approach to the design of the newly proposed structurally rigidified ureido compounds.

viciously stimulated by and then support a tumour microenvironment characterised by hypoxia and extracellular acidosis hampering therapeutic response and altering cancer cell biology[8–10]. Moreover, in this acidic and hypoxic milieu tumour cells have been reported to gain increased genetic instability and mutagenesis rate[11,12], and to become more resistant to radiation therapy and chemotherapy[13–16]. It has been amply demonstrated in several cell lines (melanoma, gastric, breast, oral, cervical, bladder, glioblastoma, pancreatic, hepatocellular, and colorectal cancer)[17–21] and in xenograft tumours *in vivo*[22,23] that selective CA IX and XII inhibitors can impair CA IX activity, triggering thus apoptosis and ferroptosis[23].

Among the several chemotypes studied for selective inhibition of tumour-associated CAs, the licenced **SLC-0111** (Figure 1), a ureido-bearing *p*-benzenesulfonamide CA IX inhibitor, is in Phase Ib/II clinical trial in combination with gemcitabine in pancreatic ductal adenocarcinoma patients with expression of CA IX (for both dose escalation and dose expansion) (https://clinicaltrials.gov/show/NCT03450018)[24]. The compound displayed promising antiproliferative effects in cancer cells transiently and chronically stimulated by extracellular acidosis, without exerting cytotoxicity in the cell population at standard pH conditions, and also enhanced ferroptosis due to the intracellular pH alkalinization reversal[23]. Moreover, it can be associated with conventional chemotherapy (dacarbazine, temozolomide, doxorubicin, 5-fluorouracil) or radiotherapy to significantly reduce tumour growth *in vivo*[25–28].

As typical of several CAIs, **SLC-0111** has the benzenesulfonamide scaffold, with the sulfonamidate zinc-binding group (ZBG) being responsible for the potent nanomolar coordination of the zinc ion present in the active site. To overcome the lack of isoform-selectivity for first and second-generation sulphonamide CAIs, we often resort to a chemical strategy, known as the tail approach, providing better discrimination of less conserved

regions of the enzyme and laid the groundwork for an extensive exploration of linkers between the ZBG and the tail. The insertion of a cyclic urea substituent on the phenyl ring of the benzenesulfonamide scaffold allows the entire molecule to better allocate within the enzymatic CA cavities proving a flexible interconnection with respect to the carboxyamido and sulphonamide groups[29–31]. Moreover, the urea functionality displays a high degree of rotational freedom, thus not blocking the molecule into a too much rigid system. Furthermore, attempts to partially restrict this structural feature were performed by designing derivatives bearing an OH group in proximity (*ortho*) to the benzenesulfonamide to form a stable intramolecular five-membered ring by H-bond with the ureido NH moiety[32]. The resulting conformationally restricted ureas (Figure 1) provided a preferential rotational isomer to interact within the CAs active sites displaying selectivity towards tumour-associated isoforms. However, when the urea was incorporated into the cyclic imidazolidin-2-one, leading to the structurally rigidified compound **SLC-149** (Figure 1), a reduction of isoform selectivity was observed compared to **SLC-0111** and some of its congeners[33].

To better explore the chemical space within the ureido benzenesulfonamide scaffold and to study the feasibility of the synthetic scheme to a larger number of derivatives, we attempted to synthesise a library of compounds characterised by: (i) a primary benzenesulfonamide as ZBG; (ii) an imidazolidin-2-one linker in *para* or *meta* position with respect to the sulphonamide function; (iii) a tail characterised by chemical diversity in terms of electronic and steric effects (aliphatic chains, differently substituted aryl groups, benzyl moieties) (Figure 1). The insertion of the cyclic ureido moiety, already reported by Zhang[34] and by Mboge et al.[33], resulted in particular interest, both from the chemical and pharmacological viewpoints, as controversial results were claimed in some recent works[33], according to which sulphonamides, such as **SLC-149** and
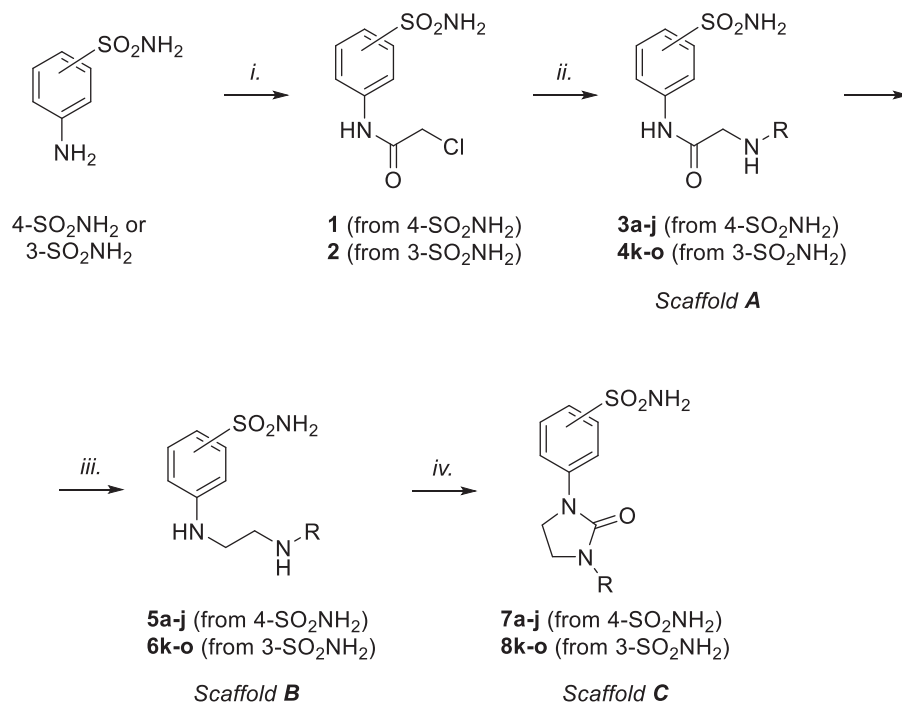
Scheme 1. General synthetic approach to prepare compounds libraries endowed with scaffolds **A**, **B**, and **C**. For R substituents, please refer to Table 1. Reagents and conditions: (i) chloroacetyl chloride, dry acetone, N_2, 0 °C, 0.5 h; (ii) for **3** and **4**: appropriately substituted aniline, KI, sealed tube, dry THF, N_2, 110 °C, 24 h; for **3i**: 2-amino-6-methylpyridine, dry TEA, abs EtOH, N_2, ref., 24 h; for **3j**: benzylamine, dry TEA, dry ACN, N_2, 24 h; for **3a**, **3b**, and **4k**: *n*-butylamine or *i*-propylamine, KI, dry THF, N_2, 24 h; (iii) for **5b,c,e,f,g,h** and **6l**: 1 M BH_3·THF, dry THF, N_2, r.t., 24 h; for **5a,d,i,j** and **6k,m,n,o**: $LiAlH_4$, dry THF, N_2, 0–70 °C, 24 h; iv. triphosgene, dry TEA, dry THF, N_2, r.t., 2 h.

congeners do not show antiproliferative activity and that the CA IX in the used cell lines does not possess a catalytic role in hypoxic tumours[33].

2. Results and discussion

2.1. Rationale of the work: design and synthesis

The preparation of ureido compounds (referred to scaffold **C** in Scheme 1) required the synthesis of amido (scaffold **A**) and amino (scaffold **B**) intermediates, as described in the following paragraphs. The different chemo-physical properties and rigidity of these scaffolds encouraged us to investigate their inhibitory activity profile against hCAs and, in particular, how the change in flexibility could affect the interaction with the target enzymes. Thus, all the final compounds and their corresponding intermediates were tested *in vitro* against two ubiquitous isoforms (hCA I and hCA II) and two membrane-anchored isoforms (hCA IX and hCA XII) to assess selectivity and inhibitory potency. In this work, we report the synthesis and characterisation of new sulphonamide ureido derivatives and report their antiproliferative activity *in vitro* on tumour cells representing glioblastoma, pancreatic, and breast cancer. The whole library of sulphonamides was obtained by a high-yielding multi-step synthetic approach, adapting previously reported pathways[34,35], as reported in Scheme 1.

Both the *para-* and *meta*-series were obtained through the same synthetic strategy by using the commercially available 4- or 3-aminobenzenesulfonamide, respectively. Their anilino groups were reacted with chloroacetyl chloride in dry acetone, furnishing the chloroacetamides **1** and **2**, respectively. Then, a nucleophilic substitution with the appropriate aniline or amine yielded derivatives **3–j** and **4k–o**, endowed with an amido scaffold **A**. Some changes in reaction conditions were required to furnish the whole set of amido compounds.

In brief, compounds **3a,b** and **4k**, endowed with aliphatic amine tails, were obtained in Finkelstein-like conditions by using potassium iodide in tetrahydrofuran (THF) at reflux, while, higher temperatures up to 110 °C were required for the anilino-bearing compounds. Otherwise, the same protocols resulted to be ineffective in preparing compounds **3i** and **3j**, bearing substituted pyridine and benzyl functions, respectively. Thus, we resorted to a traditional reaction with triethylamine (TEA) as a base. The amino derivatives **5a–j** and **6k–o** (scaffold **B**) were obtained by reducing the corresponding amides by using borane in the THF complex or lithium aluminium hydride. In the end, final compounds **7a–j** and **8k–o** (scaffold **C**) were afforded through a one-pot two-steps carbamoylation and intramolecular carbamoyl chloride-amino coupling *via* triphosgene and TEA as a base.

2.2. In vitro inhibition of human CAs and preliminary SARs consideration

The inhibition profiles for sulphonamides of scaffolds **A**, **B**, and **C** and the reference acetazolamide (**AAZ**) against the physiologically relevant hCAs I, II, IX, and XII isoforms were determined through the stopped-flow CO_2 hydrase assay[36] and are reported in Table 1.

Observing the reported data, several structure-activity relationship (SAR) considerations can be done based on the specific isoforms, the selectivity, and the chemical structures:

i. Almost all the synthesised derivatives show a nanomolar inhibitory activity against hCA I, which was found higher than the reference compound **AAZ** in some cases. Among the amido compounds (scaffold **A**) with the sulphonamide function in *para*, the phenyl derivative **3c** shows a moderate-high activity that is partially increased with the introduction of chlorine (**3g**), bromine (**3e**), or iodine (**3d**) atoms in C4 or

Table 1. Inhibition data of all the synthesised sulphonamides and reference compound acetazolamide (**AAZ**) on hCA I, II, IX, and XII isoforms through the stopped-flow CO_2 hydrase assay.

Cpd	Scaffold	Series	R	K_I hCA I [nM]	hCA II [nM]	hCA IX [nM]	hCA XII [nM]
3a	A	p-	i-propyl	92.0	26.6	32.8	140.0
3b	A	p-	n-butyl	160.5	8.4	355.3	171.3
3c	A	p-	phenyl	62.6	3.2	253.7	159.6
3d	A	p-	2-fluorophenyl	18.4	4.8	22.0	95.6
3e	A	p-	2-bromophenyl	29.8	3.0	341.8	161.0
3f	A	p-	4-tolyl	6.6	82.4	209.2	164.3
3g	A	p-	4-chlorophenyl	16.7	6.0	72.1	47.2
3h	A	p-	4-iodophenyl	>1000	909.3	68.0	174.7
3i	A	p-	6-methylpyridin-2-yl	15.3	4.7	38.3	162.3
3j	A	p-	benzyl	26.5	5.0	52.7	94.3
4k	A	m-	n-butyl	83.7	37.4	324.4	136.8
4l	A	m-	phenyl	443.3	35.5	302.2	152.3
4m	A	m-	2-bromophenyl	20.3	86.0	46.1	139.5
4n	A	m-	4-tolyl	86.4	8.2	66.7	158.0
4o	A	m-	4-chlorophenyl	268.7	32.4	72.1	47.2
5a	B	p-	i-propyl	896.0	337.7	25.7	85.3
5b	B	p-	n-butyl	538.1	82.2	64.8	119.1
5c	B	p-	phenyl	25.4	7.2	302.1	180.4
5d	B	p-	2-fluorophenyl	75.3	8.2	25.7	141.6
5e	B	p-	2-bromophenyl	939.2	908.0	380.5	160.5
5f	B	p-	4-tolyl	9.7	3.1	63.4	175.4
5g	B	p-	4-chlorophenyl	39.0	47.0	224.4	149.0
5h	B	p-	4-iodophenyl	786.6	645.8	204.7	153.2
5i	B	p-	6-methylpyridin-2-yl	87.0	31.4	47.4	170.1
5j	B	p-	benzyl	169.3	32.7	61.7	161.1
6k	B	m-	n-butyl	150.7	43.2	475.7	160.0
6l	B	m-	phenyl	7.0	4.1	52.4	166.7
6m	B	m-	2-bromophenyl	7.6	3.3	62.7	175.3
6n	B	m-	4-tolyl	>1000	900.7	411.8	166.7
6o	B	m-	4-chlorophenyl	345.7	15.7	57.1	168.0
7a	C	p-	i-propyl	8.5	3.2	67.6	42.5
7b	C	p-	n-butyl	603.5	423.0	483.0	82.0
7c	C	p-	phenyl	54.4	4.3	673.3	20.0
7d	C	p-	2-fluorophenyl	7.8	3.1	68.1	25.1
7e	C	p-	2-bromophenyl	6.2	3.4	203.1	8.7
7f	C	p-	4-tolyl	16.1	3.7	504.0	70.6
7g	C	p-	4-chlorophenyl	194.3	46.3	557.3	38.3
7h	C	p-	4-iodophenyl	92.7	13.0	477.3	54.0
7i	C	p-	6-methylpyridin-2-yl	54.6	7.2	300.0	51.4
7j	C	p-	benzyl	8.0	3.1	502.0	67.2
8k	C	m-	n-butyl	36.3	8.0	400.0	83.2
8l	C	m-	phenyl	60.6	31.1	607.6	75.4
8m	C	m-	2-bromophenyl	8.0	54.4	68.2	81.2
8n	C	m-	4-tolyl	461.6	500.0	559.2	93.4
8o	C	m-	4-chlorophenyl	30.3	84.1	468.0	>10000
AAZ (Ref. Compound)				250	12.1	25.7	5.7

K_I values are reported as means of three independent experiments by a stopped-flow technique. Errors are in the range of ±5–10% of the reported values. Acetazolamide (**AAZ**) was used as a reference control in these assays. Compounds are presented based on the molecular scaffold (**A**, amide; **B**, amine, and **C**, urea) and the (*meta-* or *para-*) position with respect to the benzenesulfonamide core.

C2. Conversely, methyl (**3f**) and iodo (**3h**) substituents on the phenyl ring result to confer the best and the worst inhibitory activities, respectively, to the library. By comparing the same tails in the *meta*-series, an overall increase in the K_I values is observed, except for derivatives **4m** and **4k**. The switching from amide to amine (scaffold **B**) and the consequent decrease in structural rigidity seems to provoke significant changes in the SARs based on the molecular tails, with the exception of the iodophenyl derivative **5h** which is still among the less active derivatives. The *para*-series with alkyl substituents (**5b** and **5a**, bearing n-butyl and i-propyl groups, respectively) exerts a lower activity than **AAZ**, whereas differences can be noticed as regards the substituted phenyl derivatives. In fact, the insertion of a methyl group in C4 (**5f**) causes an increase in affinity with respect to the unsubstituted phenyl ring of **5c** *meta*-series, while the presence of a halogen atom overall worsens the inhibitory profile of such

compounds. Although the 4-chloro (**5g**) and 2-fluoro (**5d**) substituents still maintain a good inhibitory activity on hCA I, higher than that of **AAZ**, the molecules functionalised with 4-iodo (**5h**) and 2-bromo (**5e**) phenyl groups inhibit hCA I with high-nanomolar concentrations, due to their bigger size. An opposite trend was recorded for the *meta*-series: sulphonamides **6l** and **6m**, bearing phenyl and 2-bromophenyl rings, respectively, are the best compounds in terms of activity, whereas the 4-tolyl derivative **6n** is totally inactive. In the end, among the cyclic ureas (scaffold **C**), 2-halophenyl (**7e** and **7d**) and benzyl (**7j**) along with i-propyl group (**7a**) are the best substituents for the *para*-series, while lower activities were noticed for the *meta*-series, except for the highly potent 2-bromophenyl derivative (**8m**).

ii. K_I values on hCA II reveal low nanomolar activities for the amido and urea derivatives (scaffolds **A** and **C**, respectively) of the *para*-series, following almost the same trend of data

collected for the human isoform I. This could suggest that flexibility is not well-tolerated and causes a reduction in the enzyme inhibition for these derivative libraries. In general, apart from phenyl derivatives functionalised with the electron donor methyl group (3f) and the big nucleus of the iodine atom (3h), all the *para*-substituted compounds bearing aromatic rings possess a relevant activity on hCA II, with K_I values ranging from 3.0 to 6.0 nM. The aliphatic tailed derivative 3b also shows a good inhibitory profile, while among *meta*-benzenesulfonamides, interesting results were shown only by compound 4n. Observing data on the amino compounds (scaffold B), the phenyl ring seems to positively contribute to the inhibitory properties of both the *para*- and *meta*-series, while opposite results were obtained for the 4-tolyl (5f and 6n) and 2-bromophenyl (5e and 6m) derivatives. In fact, while 5f belonging to the *para*-series and the *meta*-derivative 6m are very potent inhibitors, the corresponding isomers 6n and 5e exert low activity on hCA II, suggesting the relevant role that the steric hindrance has in the affinity to this enzyme. The *para*-series with scaffold C emerged for very low K_I values, apart from the 4-chlorophenyl-bearing (7h) and the aliphatic tailed (7b) derivatives.

iii. Inhibition data against hCA IX are in the low-medium nanomolar range. In general, the linear precursors (scaffolds A and B) appear to have a better inhibitory profile towards this isoform than the corresponding ureido derivatives (scaffold C). In particular, the most active compounds belonging to scaffold A are: 3d, 3i, 3a, and 4m, while for scaffold B they are: 5i, 5d, and 5a. It can therefore be noted that, both in the presence of the amide and diethylamine moieties, the best substituents are the isopropyl (3a, 5a), the 2-halosubstituted phenyl ring with the fluorine (3d, 5d) or bromine (4m) atoms or the presence of 6-methylpyridin-2-yl group (3i, 5i). The same trend is noticed for ureido compounds 7a, 7d, and 8m.

iv. Regarding hCA XII enzymatic activity, the compounds were very potent nanomolar inhibitors *in vitro* (except compound 8o), without any marked difference between the *meta* and the *para* series. Scaffolds A and B are equipotently providing several promising compounds for further development. The most important result is the enhancement of the hCA XII inhibitory activity after cyclisation of the ureidic linker. Indeed, all compounds (except 8o) displayed K_I values inferior to 93.4 nM achieving 8.7 nM for compound 7e. The sulphonamide group was preferred when in the *para* position.

v. Collectively, more satisfactory data are obtained from the molecules with scaffold C, therefore with a cyclic ureidic portion, rather than from the ureidic and ethylamine portions (scaffolds A and B). In fact, among amido derivatives (scaffold A), the only ones endowed with K_I values below 100 nM are those with the 4-chlorophenyl portion both in the *para* (3g) and *meta* (4o) position, the 2-fluorophenyl ring (3e), and the benzyl moiety (3j). Scaffold B-bearing most active molecule is 5a, with an isopropyl portion, while among the ureido compounds (scaffold C), all the derivatives showed a K_I lower than 100 nM, with the exception of the compound 8o. In detail, compound 7e, characterised by a 2-bromophenyl portion in the *para* position with respect to the sulphonamide function, is the one that exerts a similar activity to that of the reference standard AAZ.

2.3. Evaluation of benzenesulfonamide CAIs effects on glioblastoma cancer cells

To evaluate the effect of CAIs in human cancer cells, the expression of CA IX was first evaluated by quantitative PCR in three different glioblastoma cell lines cultured in normoxic and hypoxic (1% O_2, 5% CO_2, and 94% N_2) conditions for 24 h. As shown in Figure 2, mRNA levels of CA IX are significantly increased after exposure to hypoxia for 24 h.
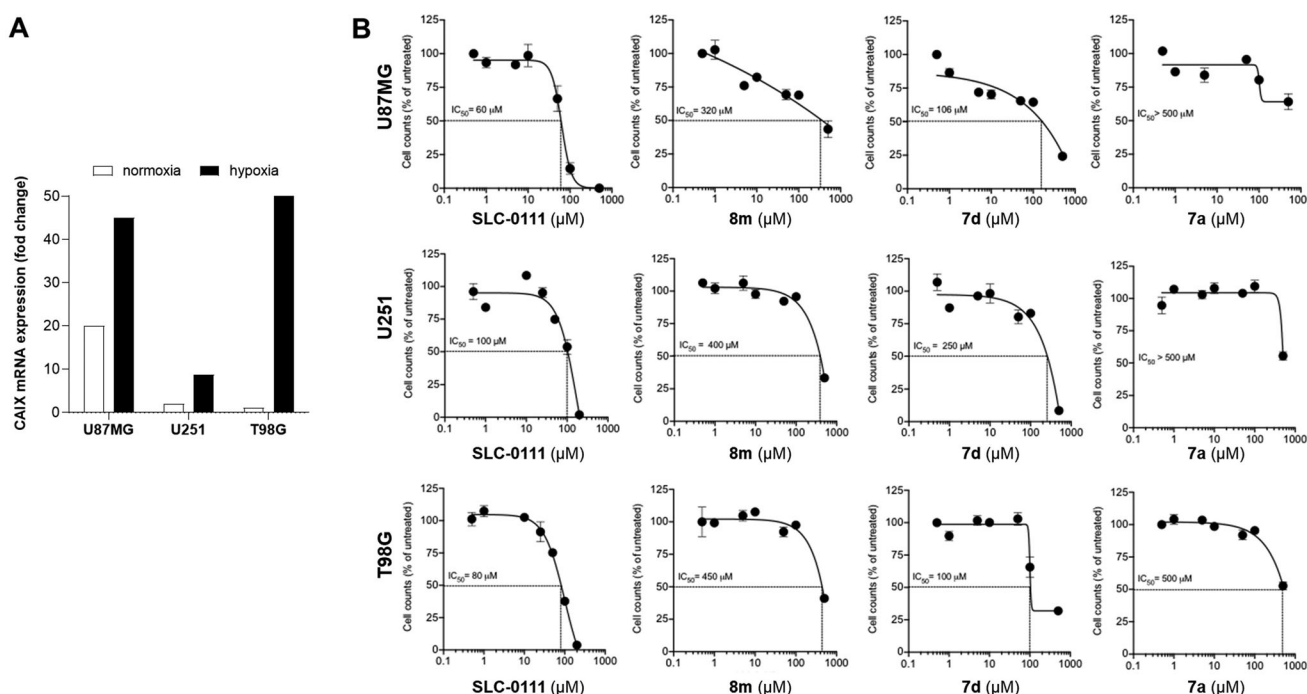
Figure 2. (A) Gene expression levels (mRNA) of CA IX in glioblastoma cancer cells under normoxic or hypoxic conditions and (B) cell proliferation of these cells treated with compounds 8m, 7d, 7a, or SLC-0111 (cell count is referred to the untreated/control considered as 100%).
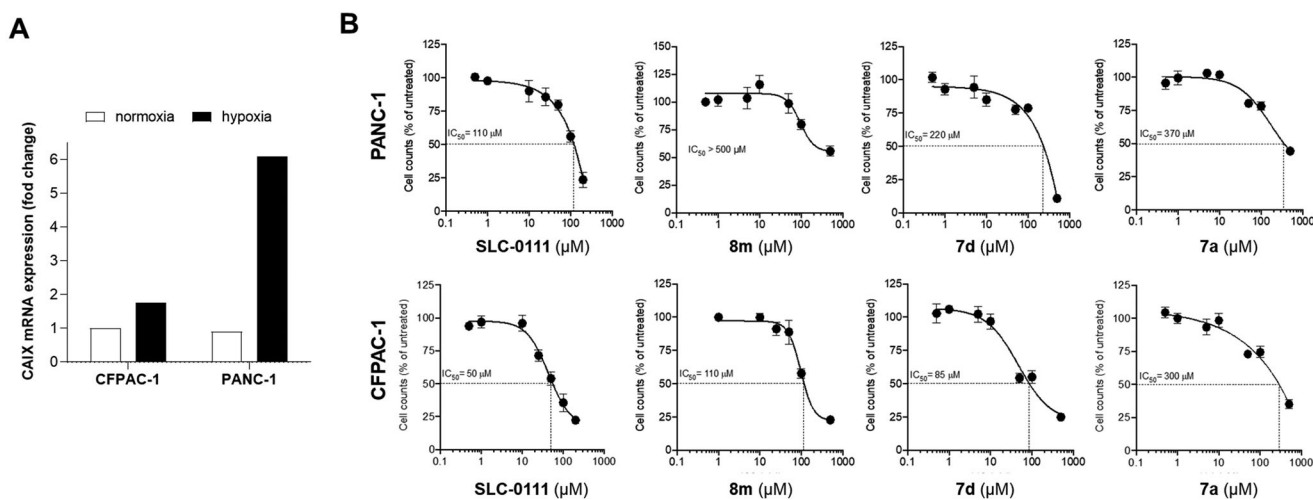
Figure 3. (A) Gene expression levels (mRNA) of *CA IX* in pancreatic cancer cells under normoxic or hypoxic conditions and (B) cell proliferation of these cells treated with compounds **8m**, **7d**, **7a**, or **SLC-0111** (cell count is referred to the untreated/control considered as 100%).
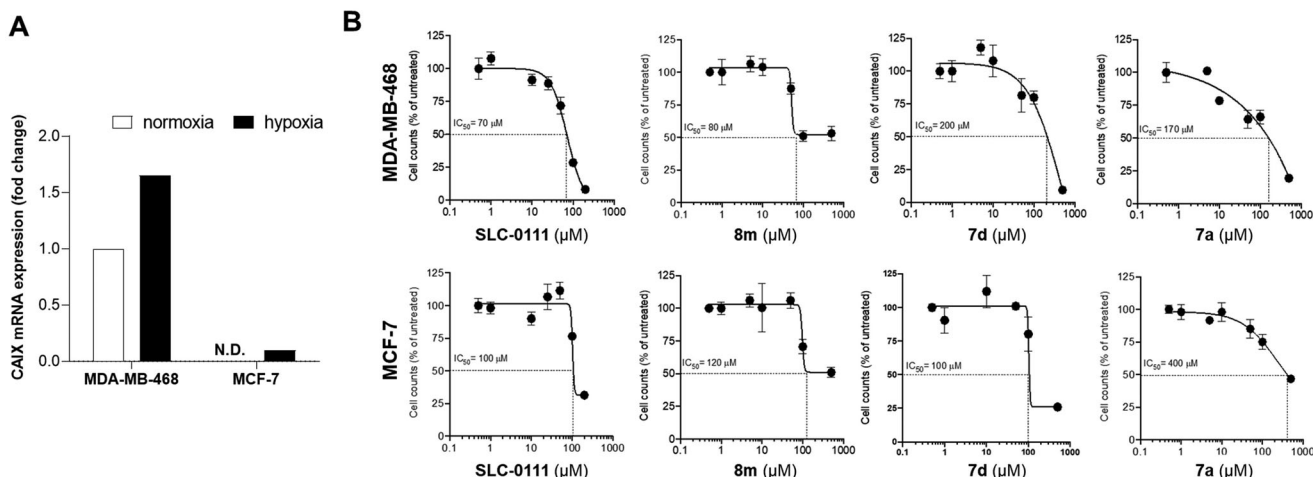
Figure 4. (A) Gene expression levels (mRNA) of *CA IX* in breast cancer cells under normoxic or hypoxic conditions and (B) cell proliferation of these cells treated with compounds **8m**, **7d**, **7a**, or **SLC-0111** (cell count is referred to the untreated/control considered as 100%).

Then, we evaluated the efficacy of the three ureido CA IX inhibitors, as representatives of the whole derivatives library with scaffold **C**, **7a**, **7d**, and **8m** to inhibit the proliferation of these glioblastoma cells after 72 h of treatment in hypoxia. To compare the results of the experiment, we also tested **SLC-0111** as a reference compound. As shown in Figure 2, the clinical grade compound **SLC-0111** was effective in reducing the proliferation of U87MG, U251, and T98G cell lines, with an IC_{50} ranging from 60 to 100 μM. Interestingly, even if less effective than **SLC-0111**, all the three compounds exhibited anti-proliferative activity, compound **7d** resulting the most effective in comparison with compounds **8m** and **7a**, with an IC_{50} ranging from 100 to 250 μM.

These data suggest that glioblastoma cells are sensitive to the inhibition of CA IX and that compound **7d** has a promising anti-proliferative effect in this tumour context.

2.4. Evaluation of CAIs effects on pancreatic cancer cells

The expression levels of *CA IX* were assessed in two cell lines of pancreatic cancer (CF-PAC-1 and PANC-1 cells) under hypoxic conditions, revealing a significant upregulation of the gene expression (Figure 3).

As shown in Figure 3 all the investigated CAIs (**7a**, **7d**, and **8m**) were efficacious in reducing pancreatic cancer cell proliferation, compound **7d** resulting the most effective with an IC_{50} of 85 μM on CFPAC-1 cells and 220 μM on PANC-1 cells. Indeed, the reference compound **SLC-0111** resulted to be the most effective with an IC_{50} of 50 μM on CFPAC-1 cells and 110 μM on PANC-1 cells. These data confirm the efficacy of **SLC-0111** on pancreatic cancer cells and the fact that compound **7d** has a higher effect compared to the other derivatives, also on this tumour type.

2.5. Evaluation of CAIs effects on breast cancer cells

In line with the previous experiments, we verified the expression of *CA IX* in two cell lines of breast cancer (MDA-MB-468 and MCF-7 cells) under hypoxic conditions and confirmed that in MDA-MB-468 cells there is an increase in CA IX expression, while in MCF-7 cells hypoxic conditions trigger the expression of CA IX that was undetectable in normoxia (Figure 4).

In vitro evaluation of the CAIs revealed that also in these cell lines, **SLC-0111** reduced cell proliferation with an IC_{50} of 70 μM on MDA-MB-468 and 100 μM on MCF-7 cells. Compound **7d** resulted in efficacious with an IC_{50} of 200 μM on MDA-MB-468 and of 100 μM on MCF-7 cells and, in this case, it was less effective

than compound **8m**, even if the latter does not reach total inhibition of cell growth at the higher concentration tested. In general, compound **7a** resulted to be less effective on the breast cancer cells tested.

3. Conclusion

Keeping in mind that the ureidic linker was successfully applied to the synthesis of potent CA IX and XII inhibitors, we followed a medicinal chemistry approach aimed at investigating how the cyclisation of this moiety into a rigidified imidazolidin-2-one group could impact CA inhibitory activity, isoform selectivity *in vitro*, and pharmacokinetic characteristics, considering the existing controversy in the field[33,37]. The introduction of the rigid imidazolidin-2-one linker was associated with a loss of selectivity for inhibiting CA IX and XII over CA II, but these compounds did possess interesting inhibition profiles. Thus, the three most representative compounds were assayed against several cancer cell lines under hypoxic conditions in comparison with **SLC-0111**. Enzyme inhibition results confirmed that chemical manipulation of the linker and the tail could modulate the CA activity, despite the presence of a pan-CA inhibiting zinc binding group (sulphonamide). Cell-based data confirmed the relevant antiproliferative properties of this class of CAIs, the importance of the tumour-associated CAs for tumour growth and development, and their inhibition as a fruitful strategy to hamper these diseases, reinforcing previous data[37,38] on the significant antitumor effects of this class of CA inhibitors.

4. Materials and methods

4.1. Chemistry

4.1.1. General chemistry

All anhydrous solvents and reagents were purchased from Alfa Aesar, TCI, and Merck. The synthetic reactions involving air- or moisture-sensitive chemicals were carried out under a nitrogen atmosphere using flame-dried glassware and syringe techniques to transfer the solutions. Analytical thin-layer chromatography (TLC) was performed on Merck silica gel F-254 plates. TLCs were visualised under UV light and stained with ninhydrin stain. Chromatographic separations were performed on columns packed with Merck Silica gel 60 (230–400 mesh ASTM, for flash technique) as the stationary phase. Melting points (m.p.) were measured in open capillary tubes with a Gallenkamp MPD350.BM3.5 apparatus and are uncorrected.

Nuclear magnetic resonance (^{1}H and ^{13}C NMR) spectra were recorded using a Bruker Advance III 400 MHz spectrometer at 400 and 100 MHz, respectively using DMSO-d_6 as solvent. The chemical shifts are reported in parts per million (ppm) and internally referenced to DMSO-d_6 signal at δ 2.50 and 39.0 ppm for ^{1}H and ^{13}C NMR spectra, respectively. Data are shown as follows: chemical shift, multiplicity (splitting patterns are designated as s, singlet; d, doublet; t, triplet; q, quartette; m, multiplet; brs, broad singlet; dd, doublet of doublets; ap, apparent), integration, and coupling constants (*J*) in Hertz (Hz). The correct assignment of exchangeable protons (i.e. OH and NH) was carried out using the addition of D_2O.

The high-resolution mass spectrometry (HRMS) analysis was performed using a Thermo Finnigan LTQ Orbitrap mass spectrometer coupled with an electrospray ionisation source (ESI). The HRMS analysis was performed by introducing the analyte working solution *via* syringe pump at 10 µL/min. Analyses were carried out in positive ion scanning mode and it was used a proper dwell time acquisition to achieve 60.000 units of resolution at full width at half maximum (FWHM). The elemental composition of compounds was calculated based on their measured accurate masses, accepting only results with an attribution error <5 ppm and a not integer RDB (double bond/ring equivalents) value (data not shown). Stock solutions of analytes were prepared using acetone (1.0 mg/mL) and stored at 4 °C. Then, working solutions of each analyte were prepared by dilution of the stock solutions using mQ H_2O/ACN 1/1 (*v/v*) up to a concentration of 1.0 µg/mL.

The behaviour of all the tested compounds as pan-assay interference compounds (PAINS) was examined through prediction by the SwissADME tool[39], revealing the absence of PAINS fragments (0 alert), and the online FAFDrugs4 (Free ADME-Tox Filtering Tool) program[40] (for non-fluorine-bearing compounds). Through its tool Bank-Formatter, the compound library was prepared and then screened with the three different available filters A, B, and C[41]. All the analysed compounds resulted as "accepted" by the software (FAFDrugs4, https://fafdrugs4.rpbs.univ-paris-diderot.fr/).

4.2. General procedure for compounds 1 and 2

4-Aminobenzensulfonamide **1** or 3-aminobenzensulfonamide **2** (2.00 g, 11.61 mmol, 1 eq.) and potassium carbonate (2.08 g, 15.09 mmol, 1.3 eq.) were suspended in dry acetone (20 mL) under nitrogen atmosphere and the suspension was cooled to 0 °C in an ice bath. Chloroacetyl chloride (924 µL, 11.61 mmol, 1 eq.) was added dropwise under a nitrogen atmosphere. The reaction was stirred for 30 min at room temperature, quenched with water, filtered and the filtrate was evaporated under vacuum. The product was obtained with no further purification.

4.2.1. 2-Chloro-N-(4-sulfamoylphenyl)acetamide (1)
White solid. Yield = 69%, silica gel TLC R$_f$ 0.50 (EtOAc/Hex 70% *v/v*); ^{1}H NMR (400 MHz, DMSO-d_6) δ (ppm): 7.76 (m, 4H), 7.26 (s, 2H), 4.29 (s, 2H).

4.2.2. 2-Chloro-N-(3-sulfamoylphenyl)acetamide (2)
White solid. Yield = 69%, silica gel TLC R$_f$ 0.50 (EtOAc/Hex 70% *v/v*); ^{1}H NMR (400 MHz, DMSO-d_6) δ (ppm): 10.67 (s, 1H), 8.19 (s, 1H), 7.78 (dd, 1H, *J* = 6.42 Hz), 7.57 (d, 2H, *J* = 6.42 Hz), 7.43 (s, 2H), 4.33 (s, 2H).

4.3. General procedure for compounds 3a–h and 4k–o

To a stirring solution of **1** or **2** (1.00 g, 4.02 mmol, 1 eq.) in dry THF in a tube, KI (100.0 mg, 0.60 mmol, 0.15 eq.) for **3a–h** or (200.0 mg, 1.20 mmol, 0.30 eq.) for **4k–o** and the appropriate amine or aniline (24.12 mmol, 6 eq.) were added at room temperature under nitrogen atmosphere. Then, the reaction mixture was heated at 110 °C for 24 h. After reaction completion, the reaction was quenched with deionised water and extracted with EtOAc three times. The combined organic layers were washed with brine, dried over anhydrous Na_2SO_4, filtered, and evaporated under vacuum. The obtained crudes were washed with diethyl ether and purified by silica gel flash column chromatography.

4.3.1. 2-(Isopropylamino)-N-(4-sulfamoylphenyl)acetamide (3a)
Red solid. Yield = 39%, silica gel TLC R$_f$ 0.10 (MeOH/DCM 15% *v/v*); ^{1}H NMR (400 MHz, DMSO-d_6) δ (ppm): 10.19 (bs, 1H), 7.82 (m,

4H), 7.28 (s, 2H), 3.37 (s, 2H), 2.79 (m, 1H), 1.05 (d, 6H, $J = 6.24$ Hz); ^{13}C NMR (100 MHz, DMSO-d_6) δ (ppm): 172.3, 142.5, 139.8, 127.8, 119.7, 51.6, 49.3, 23.6; HRMS m/z: 272.1 [M + H]$^+$.

4.3.2. 2-(Butylamino)-N-(4-sulfamoylphenyl)acetamide (3b)
Yellow solid. M.p. 167–169 °C. Yield = 96%, silica gel TLC R_f 0.15 (MeOH/DCM 15% v/v); ^{1}H NMR (400 MHz, DMSO-d_6) δ (ppm): 10.09 (bs, 1H), 7.81 (dd, 4H, $J = 8.94$ Hz, $J = 7.13$ Hz), 7.27 (s, 2H), 3.37 (s, 2H), 2.57 (d, 2H, $J = 6.89$ Hz), 1.44 (m, 2H), 1.35 (m, 2H), 0.91 (t, 3H, $J = 7.31$ Hz); ^{13}C NMR (100 MHz, DMSO-d_6) δ (ppm): 171.6, 142.0, 138.8, 127.1, 119.1, 53.4, 49.3, 32.1, 20.3, 14.3; HRMS m/z: 286.1 [M + H]$^+$.

4.3.3. 2-(Phenylamino)-N-(4-sulfamoylphenyl)acetamide (3c)
White solid. M.p. 123–125 °C. Yield =59%, silica gel TLC R_f 0.2 (MeOH/DCM 5% v/v); ^{1}H NMR (400 MHz, DMSO-d_6) δ (ppm): 10.35 (s, 1H), 7.80 (dd, 4H, $J = 9.34$ Hz, $J = 15.52$ Hz), 7.28 (s, 2H), 7.13 (t, 2H, $J = 7.44$ Hz), 6.63 (d, 3H, $J = 8.59$ Hz), 6.59 (d, 1H, $J = 5.02$ Hz), 6.03 (t, 1H, $J = 6.11$ Hz), 3.93 (d, 2H, $J = 6.16$ Hz); ^{13}C NMR (100 MHz, DMSO-d_6) δ (ppm): 171.1, 149.3, 142.8, 139.5, 129.9, 127.8, 119.9, 117.6, 113.4, 48.5; HRMS m/z: 306.1 [M + H]$^+$.

4.3.4. 2-((2-Fluorophenyl)amino)-N-(4-sulfamoylphenyl)acetamide (3d)
Pink solid. M.p. 191–193 °C. Yield = 38%, silica gel TLC R_f 0.50 (EtOAc/Hex 70% v/v); ^{1}H NMR (400 MHz, DMSO-d_6) δ (ppm): 10.40 (s, 1H), 7.80 (s, 4H), 7.27 (s, 2H), 7.08 (t, 1H, $J = 10.13$ Hz), 7.00 (t, 1H, $J = 7.67$ Hz), 6.66 (t, 2H, $J = 9.53$ Hz), 5.79 (d, 1H, $J = 6.36$ Hz), 4.01 (d, 2H, $J = 5.77$ Hz); HRMS m/z: 324.1 [M + H]$^+$.

4.3.5. 2-((2-Bromophenyl)amino)-N-(4-sulfamoylphenyl)acetamide (3e)
Black solid. Yield = 49%, silica gel TLC R_f 0.27 (MeOH/DCM 3% v/v); ^{1}H NMR (400 MHz, DMSO-d_6) δ (ppm): 10.51 (s, 1H), 7.80 (s, 4H), 7.48 (dd, 1H, $J = 8.14$ Hz, $J = 8.29$ Hz), 7.29 (s, 2H), 7.23 (t, 1H, $J = 7.35$ Hz), 6.62 (d, 2H, $J = 5.92$ Hz), 5.62 (t, 1H, $J = 6.39$ Hz), 4.08 (d, 2H, $J = 5.59$ Hz); ^{13}C NMR (100 MHz, DMSO-d_6) δ (ppm): 169.4, 145.1, 142.1, 138.9, 132.7, 129.2, 127.2, 119.2, 118.3, 112.1, 109.2, 47.3; HRMS m/z: 384.0 [M + H]$^+$.

4.3.6. N-(4-sulfamoylphenyl)-2-(p-tolylamino)acetamide (3f)
Brown solid. Yield = 51%, silica gel TLC R_f 0.20 (MeOH/DCM 5% v/v); ^{1}H NMR (400 MHz, DMSO-d_6) δ (ppm): 10.30 (s, 1H), 7.80 (dd, 4H, $J = 11.53$ Hz, $J = 15.01$ Hz), 7.27 (s, 2H), 6.94 (d, 2H, $J = 8.21$ Hz), 6.55 (d, 2H, $J = 8.21$ Hz), 5.84 (t, 1H, $J = 5.92$ Hz), 3.89 (d, 2H, $J = 5.99$ Hz), 2.18 (s, 3H); HRMS m/z: 320.1 [M + H]$^+$ in agreement with[35].

4.3.7. 2-((4-Chlorophenyl)amino)-N-(4-sulfamoylphenyl)acetamide (3g)
Purple solid. M.p. 210–212 °C. Yield = 84%, silica gel TLC R_f 0.2 (MeOH/DCM 5% v/v); ^{1}H NMR (400 MHz, DMSO-d_6) δ (ppm): 10.37 (s, 1H), 7.80 (s, 4H), 7.28 (s, 2H), 7.15 (d, 2H, $J = 8.30$ Hz), 6.64 (d, 2H, $J = 8.23$ Hz), 6.26 (bs, 1H), 3.95 (s, 2H); ^{13}C NMR (100 MHz, DMSO-d_6) δ (ppm): 170.1, 147.7, 142.2, 138.9, 129.0, 127.2, 120.2, 119.3, 114.2, 47.6, 31.1; HRMS m/z: 340.0 [M + H]$^+$ in agreement with[35].

4.3.8. 2-((4-Iodophenyl)amino)-N-(4-sulfamoylphenyl)acetamide (3h)
White solid. Yield = 58%, silica gel TLC R_f 0.15 (MeOH/DCM 5% v/v); ^{1}H NMR (400 MHz, DMSO-d_6) δ (ppm): 10.30 (s, 1H), 7.80 (dd, 4H, $J = 11.53$ Hz, $J = 15.01$ Hz), 7.27 (s, 2H), 6.94 (d, 2H, $J = 8.21$ Hz), 6.55 (d, 2H, $J = 8.21$ Hz), 5.84 (t, 1H, $J = 5.92$ Hz), 3.89 (d, 2H, $J = 5.99$ Hz); ^{13}C NMR (100 MHz, DMSO-d_6) δ (ppm): 170.8, 149.5, 142.9, 140.0, 129.9, 127.7, 119.6, 118.2, 113.4, 49.2; HRMS m/z: 431.9 [M + H]$^+$.

4.3.9. 2-(Butylamino)-N-(3-sulfamoylphenyl)acetamide (4k)
Yellow solid. Yield = 60%, silica gel TLC R_f 0.10 (MeOH/DCM 15% v/v); ^{1}H NMR (400 MHz, DMSO-d_6) δ (ppm): 10.09 (bs, 1H), 8.26 (s, 1H), 7.80 (d, 1H, $J = 5.00$ Hz), 7.54 (d, 2H, $J = 5.90$ Hz), 7.39 (bs, 2H), 2.12 (t, 1H, $J = 7.50$ Hz), 1.45 (m, 3H), 1.36 (m, 3H), 0.91 (t, 5H, $J = 7.01$ Hz); ^{13}C NMR (100 MHz, DMSO-d_6) δ (ppm): 171.9, 145.7, 140.1, 130.5, 123.1, 121.4, 117.2, 53.9, 49.8, 32.7, 20.9, 14.9; HRMS m/z: 286.1 [M + H]$^+$.

4.3.10. 2-(Phenylamino)-N-(3-sulfamoylphenyl)acetamide (4l)
Brown solid. M.p. 181–183 °C. Yield = 35%, silica gel TLC R_f 0.20 (MeOH/DCM 5% v/v); ^{1}H NMR (400 MHz, DMSO-d_6) δ (ppm): 10.32 (s, 1H), 8.22 (s, 1H), 7.82 (m, 1H), 7.53 (apt, 2H, $J = 7.67$ Hz), 7.38 (s, 2H), 7.13 (t, 2H, $J = 7.44$ Hz), 6.62 (apt, 3H, $J = 8.65$ Hz), 6.05 (t, 1H, $J = 6.10$ Hz), 3.92 (d, 2H, $J = 6.23$ Hz); ^{13}C NMR (100 MHz, DMSO-d_6) δ (ppm): 170.9, 149.3, 145.7, 140.2, 130.5, 130.0, 123.2, 121.5, 117.6, 117.4, 113.4, 48.4; HRMS m/z: 306.1 [M + H]$^+$.

4.3.11. 2-((2-Bromophenyl)amino)-N-(3-sulfamoylphenyl)acetamide (4m)
Purple solid. Yield = 49%, silica gel TLC R_f 0.33 (MeOH/DCM 5% v/v); ^{1}H NMR (400 MHz, DMSO-d_6) δ (ppm): 10.49 (s, 1H), 8.22 (s, 1H), 7.78 (s, 1H), 7.54 (d, 2H, $J = 5.24$ Hz), 7.48 (d, 1H, $J = 8.14$ Hz), 7.42 (s, 1H), 7.39 (s, 2H), 7.22 (t, 1H, $J = 7.65$ Hz), 6.61 (d, 1H, $J = 7.47$ Hz), 5.64 (t, 1H, $J = 5.43$ Hz), 4.06 (d, 2H, $J = 5.53$ Hz); ^{13}C NMR (100 MHz, DMSO-d_6) δ (ppm): 168.5, 146.8, 139.9, 138.8, 132.4, 128.5, 127.0, 124.8, 119.8, 115.7, 114.5, 54.5; HRMS m/z: 384.0 [M + H]$^+$.

4.3.12. N-(3-sulfamoylphenyl)-2-(p-tolylamino)acetamide (4n)
Yellow solid. Yield = 49%, silica gel TLC R_f 0.38 (MeOH/DCM 5% v/v); ^{1}H NMR (400 MHz, DMSO-d_6) δ (ppm): 10.27 (s, 1H), 8.21 (s, 1H), 7.81 (s, 1H), 7.45 (d, 4H, $J = 10.13$ Hz), 6.95 (d, 2H, $J = 7.18$ Hz), 6.55 (d, 2H, $J = 8.28$ Hz), 5.84 (d, 1H, $J = 6.53$ Hz), 3.88 (d, 2H, $J = 6.67$ Hz), 2.17 (d, 3H, $J = 7.41$ Hz); ^{13}C NMR (100 MHz, DMSO-d_6) δ (ppm): 171.1, 147.0, 145.7, 140.2, 130.5, 130.4, 126.0, 123.2, 121.4, 117.3, 113.5, 48.8, 21.1; HRMS m/z: 320.1 [M + H]$^+$.

4.3.13. 2-((4-Chlorophenyl)amino)-N-(3-sulfamoylphenyl)acetamide (4o)
Purple solid. M.p. 148–150 °C. Yield = 57%, silica gel TLC R_f 0.40 (MeOH/DCM 5% v/v); ^{1}H NMR (400 MHz, DMSO-d_6) δ (ppm): 10.34 (s, 1H), 8.21 (s, 1H), 7.80 (s, 1H), 7.54 (s, 2H), 7.38 (s, 2H), 7.15 (d, 2H, $J = 8.48$ Hz), 6.63 (d, 2H, $J = 8.44$ Hz), 6.27 (bs, 1H), 3.92 (d, 2H, $J = 5.71$ Hz); ^{13}C NMR (100 MHz, DMSO-d_6) δ (ppm): 170.5, 148.3, 145.7, 140.2, 130.5, 129.7, 123.2, 121.5, 120.9, 117.4, 114.8, 48.3; HRMS m/z: 340.0 [M + H]$^+$.

4.4. Synthesis of 2-((6-methylpyridin-2-yl)amino)-N-(4-sulfamoylphenyl)acetamide (3i)

To a stirring solution of **2.1a** (1 g, 4.02 mmol, 1 eq.) in abs EtOH (25 mL), 6-methylpyridin-2-amine (434.51 mg, 4.018 mmol, 1 eq.) and dry TEA (0.56 mL, 4.02 mmol, 1 eq.) were added. Then, the reaction mixture was stirred at 78 °C for 16 h. After completion, 1 M HCl was added till neutralisation and the mixture was extracted with EtOAc three times. The combined organic layers were washed with brine, dried over anhydrous Na_2SO_4, filtered, and evaporated under a vacuum. The product was obtained with no further purification. Red solid. Yield = 46%, silica gel TLC R_f 0.65 (EtOAc/Hex 70% v/v); ^{1}H NMR (400 MHz, DMSO-d_6) δ (ppm): 10.68 (s, 1H), 7.81 (m, 4H), 7.33 (s, 2H), 7.27 (t, 1H, $J = 7.56$ Hz), 6.36 (d, 1H, $J = 7.16$ Hz), 6.26 (d, 1H, $J = 8.30$ Hz), 4.34 (s, 2H), 2.24 (s, 3H); ^{13}C NMR (100 MHz, DMSO-d_6) δ (ppm): 157.4, 151.0, 142.5, 128.5, 127.7, 119.7, 112.3, 109.1, 106.8, 46.2, 21.7; HRMS m/z: 321.1 [M + H]$^+$.

4.5. Synthesis of 2-(benzylamino)-N-(4-sulfamoylphenyl)acetamide (3j)

1 (1.00 g, 4.02 mmol, 1 eq.) was dissolved in dry ACN (20 ml) and then benzylamine (0.48 mL, 4.42 mmol, 1.1 eq.) and dry TEA (0.73 mL, 5.22 mmol, 1.3 eq.) were added under nitrogen atmosphere. The reaction was stirred at 82 °C for 16 h. After cooling, the reaction was quenched with water and filtered. The obtained solid was washed several times with Et_2O. White solid. M.p. 195–1978 °C. Yield = 39%, silica gel TLC R_f 0.45 (MeOH/DCM 5% v/v); ^{1}H NMR (400 MHz, DMSO-d_6) δ (ppm): 10.20 (s, 1H), 7.81 (m, 4H), 7.37 (m, 4H), 7.28 (s, 2H), 3.78 (s, 2H), 3.35 (s, 2H); ^{13}C NMR (100 MHz, DMSO-d_6) δ (ppm): 171.3, 142.1, 140.7, 138.8, 128.7, 128.5, 127.2, 127.1, 119.2, 53.0, 52.5; HRMS m/z: 329.1 [M + H]$^+$.

4.6. General procedure for compounds 5b,c,e,f,g,h, and 6l

To a stirring solution of the suitable amide derivative (**3b,c,e,f,g,h,** or **4l**) (150.0 mg, 0.47 mmol, 1 eq.) in dry THF (20 mL), 1 M BH_3.THF complex (3.25 mL, 3.09 mmol, 6.5 eq.) was added at room temperature under nitrogen atmosphere. Then, the mixture was stirred at 110 °C for 24 h. After cooling, the reaction mixture was quenched with deionised water, and extracted with EtOAc three times. The combined organic layers were washed with brine, dried over anhydrous Na_2SO_4, filtered, and evaporated under vacuum. The reaction crudes were purified by silica gel flash column chromatography.

4.6.1. 4-((2-(Butylamino)ethyl)amino)benzenesulfonamide (5b)

Yellow solid. M.p. 165–167 °C. Yield = 43%, silica gel TLC R_f 0.16 (MeOH/DCM 15% v/v); ^{1}H NMR (400 MHz, DMSO-d_6) δ (ppm): 7.81 (m, 4H), 7.28 (s, 2H), 3.51 (s, 4H), 1.81 (s, 1H), 1.45 (m, 2H), 1.37 (m, 2H), 1.27 (m, 2H), 0.93 (t, 3H, $J = 6.04$ Hz); ^{13}C NMR (100 MHz, DMSO-d_6) δ (ppm): 152.6, 130.9, 128.4, 111.8, 49.9, 49.2, 43.6, 32.9, 21.1, 15.0; HRMS m/z: 272.1 [M + H]$^+$.

4.6.2. 4-((2-(Phenylamino)ethyl)amino)benzenesulfonamide (5c)

White solid. Yield = 33%. silica gel TLC R_f 0.50 (EtOAc/Hex 70% v/v); ^{1}H NMR (400 MHz, DMSO-d_6) δ (ppm): 7.55 (d, 2H, $J = 8.42$ Hz), 7.11 (t, 2H, $J = 7.64$ Hz), 6.40 (s, 2H), 6.68 (s, 2H, $J = 8.61$ Hz), 6.62 (d, 2H, $J = 7.91$ Hz), 6.57 (t, 2H, $J = 7.55$ Hz), 6.46 (apt, 1H, $J = 7.13$ Hz); ^{13}C NMR (100 MHz, DMSO-d_6) δ (ppm): 152.4, 149.7,

131.2, 130.0, 128.5, 116.9, 113.2, 111.9, 42.9, 42.8; HRMS m/z: 292.1 [M + H]$^+$.

4.6.3. 4-((2-((2-Bromophenyl)amino)ethyl)amino)benzenesulfonamide (5e)

Brown solid. Yield = 69%, silica gel TLC R_f 0.24 (MeOH/DCM 3% v/v); ^{1}H NMR (400 MHz, DMSO-d_6) δ (ppm): 7.55 (d, 2H, $J = 8.77$ Hz), 7.44 (d, 1H, $J = 7.82$ Hz), 7.22 (t, 1H, $J = 8.06$ Hz), 6.96 (s, 2H), 6.78 (d, 1H, $J = 7.82$ Hz), 6.70 (d, 2H, $J = 8.77$ Hz), 6.56 (t, 2H, $J = 6.54$ Hz), 5.30 (apt, 1H, $J = 5.45$ Hz), 4.36 (s, 4H); ^{13}C NMR (100 MHz, DMSO-d_6) δ (ppm): 144.3, 143.1, 138.9, 132.7, 130.4, 129.5, 119.2, 117.3, 111.1, 109.2, 47.3, 42.7; HRMS m/z: 370.0 [M + H]$^+$.

4.6.4. 4-((2-(p-Tolylamino)ethyl)amino)benzenesulfonamide (5f)

Brown solid. Yield = 38%, silica gel TLC R_f 0.50 (EtOAc/Hex 70% v/v); ^{1}H NMR (400 MHz, DMSO-d_6) δ (ppm): 7.54 (d, 2H, $J = 8.81$ Hz), 6.93 (d, 4H, $J = 6.66$ Hz), 6.67 (d, 2H, $J = 8.81$ Hz), 6.54 (d, 2H, $J = 8.33$ Hz), 6.45 (bs, 1H), 5.44 (s, 1H), 3.30 (d, 2H, $J = 5.34$ Hz), 3.23 (d, 2H, $J = 5.34$ Hz), 2.18 (s, 3H); HRMS m/z: 306.1 [M + H]$^+$ in agreement with[34].

4.6.5. 4-((2-((4-Chlorophenyl)amino)ethyl)amino)benzenesulfonamide (5g)

Black solid. M.p. 178–180 °C. Yield = 53%, silica gel TLC R_f 0.23 (MeOH/DCM 3% v/v); ^{1}H NMR (400 MHz, DMSO-d_6) δ (ppm): 7.55 (d, 2H, $J = 8.67$ Hz), 7.13 (d, 2H, $J = 8.52$ Hz), 6.95 (s, 2H), 6.67 (d, 2H, $J = 8.86$ Hz), 6.62 (d, 2H, $J = 8.86$ Hz), 6.46 (t, 1H, $J = 5.22$ Hz), 5.91 (t, 1H, $J = 5.21$ Hz), 3.29 (t, 2H, $J = 5.65$ Hz), 3.25 (t, 2H, $J = 5.72$ Hz); ^{13}C NMR (100 MHz, DMSO-d_6) δ (ppm): 152.4, 148.6, 131.3, 129.7, 128.5, 120.1, 114.5, 111.9, 43.0, 42.7; HRMS m/z: 326.1 [M + H]$^+$.

4.6.6. 4-((2-((4-Iodophenyl)amino)ethyl)amino)benzenesulfonamide (5h)

White solid. Yield = 66%, silica gel TLC R_f 0.24 (MeOH/DCM 3% v/v); ^{1}H NMR (400 MHz, DMSO-d_6) δ (ppm): 7.54 (m, 4H), 7.38 (d, 1H, $J = 8.80$ Hz), 6.96 (bs, 2H), 6.68 (m, 4H), 6.49 (d, 1H, $J = 8.80$ Hz), 3.76 (t, 4H, $J = 6.24$ Hz); ^{13}C NMR (100 MHz, DMSO-d_6) δ (ppm): 152.6, 148.8, 131.7, 130.1, 129.5, 120.1, 114.6, 111.7, 43.1, 42.9; HRMS m/z: 418.0 [M + H]$^+$.

4.6.7. 3-((2-(Phenylamino)ethyl)amino)benzenesulfonamide (6l)

Brown solid. M.p. 146–148 °C. Yield = 51%, silica gel TLC R_f 0.43 (EtOAc/Hex 50% v/v); ^{1}H NMR (400 MHz, DMSO-d_6) δ (ppm): 7.27 (t, 1H, $J = 7.80$ Hz), 7.21 (s. 1H), 7.12 (t, 2H, $J = 7.80$ Hz), 7.06 (s, 1H), 7.01 (d, 1H, $J = 7.50$ Hz), 6.80 (dd, 1H, $J = 8.12$ Hz, $J = 6.44$ Hz), 6.63 (d, 2H, $J = 7.79$ Hz), 6.57 (t, 1H, $J = 7.18$ Hz), 6.19 (apt, 1H, $J = 5.19$ Hz), 5.66 (apt, 1H, $J = 5.19$ Hz), 3.28 (s, 4H); ^{13}C NMR (100 MHz, DMSO-d_6) δ (ppm): 150.0, 149.7, 145.9, 130.4, 130.0, 116.9, 116.1, 113.6, 113.2, 109.5, 43.1, 42.9; HRMS m/z: 292.1 [M + H]$^+$.

4.7. General procedure for compounds 5a,d,i,j and 6k,m–o

To a stirring solution of LiAlH$_4$ (192.41 mg, 5.07 mmol, 6 eq.) in dry THF (20 mL) in an ice bath (0 °C), a solution of the suitable amide derivative **3a,d,i,j** or **4k,m–o**; (0.85 mmol, 1 eq.) in dry THF (5 ml)

was added dropwise under nitrogen atmosphere. Then, the reaction mixture was stirred at 70 °C for 16 h. After cooling in an ice bath at 0 °C, the reaction was quenched with water, and the mixture was extracted with EtOAc three times. The combined organic layers were washed with brine, dried over anhydrous Na_2SO_4, filtered, and evaporated under vacuum. The reaction crudes were purified by silica gel flash column chromatography.

4.7.1. 4-((2-(Isopropylamino)ethyl)amino)benzenesulfonamide (5a)

Brown solid. Yield = 59%, silica gel TLC R_f 0.10 (MeOH/DCM 15% v/v); ^{1}H NMR (400 MHz, DMSO-d_6) δ (ppm): 7.53 (d, 2H, $J = 8.26$ Hz), 6.94 (s, 2H), 6.65 (d, 2H, $J = 8.26$ Hz), 6.36 (apt, 1H, $J = 7.40$ Hz), 3.15 (m, 2H), 2.72 (m, 2H), 1.66 (m, 1H), 1.01 (d, 6H, $J = 5.92$ Hz); ^{13}C NMR (100 MHz, DMSO-d_6) δ (ppm): 151.9, 130.4, 127.8, 111.1, 48.4, 45.9, 43.4, 23.4; HRMS m/z: 258.1 [M + H]$^+$.

4.7.2. 4-((2-((2-Fluorophenyl)amino)ethyl)amino)benzenesulfonamide (5d)

Brown solid. Yield = 30%, silica gel TLC R_f 0.35 (EtOAc/Hex 50% v/v); ^{1}H NMR (400 MHz, DMSO-d_6) δ (ppm): 7.48 (d, 2H, $J = 8.80$ Hz), 6.97 (m, 2H), 6.88 (bs, 2H), 6.73 (m, 1H), 6.62 (d, 2H, $J = 8.80$ Hz), 6.57 (m, 1H), 6.43 (t, 1H, $J = 5.2$ Hz), 5.42 (bs, 1H), 3.26 (m, 4H); HRMS m/z: 310.1 [M + H]$^+$ in agreement with[34].

4.7.3. 4-((2-((6-Methylpyridin-2-yl)amino)ethyl)amino)benzenesulfonamide (5i)

Brown oil. Yield = 38%, silica gel TLC R_f 0.40 (MeOH/DCM 10% v/v); ^{1}H NMR (400 MHz, DMSO-d_6) δ (ppm): 7.55 (d, 2H, $J = 8.68$ Hz), 7.30 (t, 1H, $J = 7.96$ Hz), 6.94 (s, 2H), 6.80 (d, 2H, $J = 8.90$ Hz), 6.57 (apt, 2H, $J = 7.23$ Hz), 6.40 (d, 1H, $J = 7.23$ Hz), 6.30 (d, 1H, $J = 7.78$ Hz), 3.29 (apt, 2H, $J = 7.10$ Hz), 2.35 (s, 3H); ^{13}C NMR (100 MHz, DMSO-d_6) δ (ppm): 148.1, 145.7, 140.8, 130.5, 129.3, 127.3, 119.0, 111.1, 103.5, 49.0, 46.8, 23.9; HRMS m/z: 307.1 [M + H]$^+$.

4.7.4. 4-((2-(Benzylamino)ethyl)amino)benzenesulfonamide (5j)

White solid. Yield = 37%, silica gel TLC R_f 0.50 (MeOH/DCM 5% v/v); ^{1}H NMR (400 MHz, DMSO-d_6) δ (ppm): 7.53 (d, 2H, $J = 8.82$ Hz), 7.35 (m, 4H), 7.25 (t, 1H, $J = 6.74$ Hz), 6.94 (s, 2H), 6.65 (d, 2H, $J = 8.72$ Hz), 6.33 (t, 1H, $J = 5.38$ Hz), 3.20 (q, 2H, $J = 6.04$ Hz), 2.73 (t, 2H, $J = 6.33$ Hz); ^{13}C NMR (100 MHz, DMSO-d_6) δ (ppm): 150.8, 140.2, 139.9, 128.5, 127.9, 127.3, 127.0, 111.1, 52.3, 49.4, 48.5; HRMS m/z: 306.1 [M + H]$^+$.

4.7.5. 3-((2-(Butylamino)ethyl)amino)benzenesulfonamide (6k)

Yellow solid. Yield = 32%, silica gel TLC R_f 0.50 (EtOAc/Hex 60% v/v); ^{1}H NMR (400 MHz, DMSO-d_6) δ (ppm): 7.25 (t, 1H, $J = 7.75$ Hz), 7.04 (s, 1H), 6.99 (d, 1H, $J = 7.51$ Hz), 6.78 (d, 1H, $J = 8.00$ Hz), 6.05 (apt, 1H, $J = 5.46$ Hz), 3.20 (s, 2H), 3.16 (m, 2H), 2.75 (t, 1H, $J = 5.96$ Hz), 2.12 (s, 2H), 1.14 (m, 2H), 1.13 (m, 2H), 0.90 (t, 3H, $J = 7.01$ Hz); ^{13}C NMR (100 MHz, DMSO-d_6) δ (ppm): 150.1, 145.9, 130.3, 115.9, 113.4, 109.4, 49.7, 48.9, 43.5, 32.5, 20.9, 14.9; HRMS m/z: 272.1 [M + H]$^+$.

4.7.6. 3-((2-((2-Bromophenyl)amino)ethyl)amino)benzenesulfonamide (6m)

Brown solid. M.p. 172–174 °C. Yield = 49%, silica gel TLC R_f 0.25 (EtOAc/Hex 40% v/v); ^{1}H NMR (400 MHz, DMSO-d_6) δ (ppm): 7.44 (d, 1H, $J = 7.94$ Hz), 7.27 (m, 2H), 7.19 (s, 2H), 7.07 (s, 1H), 7.01 (d, 2H, $J = 7.10$ Hz), 6.80 (t, 2H, $J = 9.61$ Hz), 6.57 (t, 1H, $J = 7.40$ Hz), 6.28 (t, 1H, $J = 5.65$ Hz), 5.28 (t, 1H, $J = 5.65$ Hz), 3.40 (t, 2H, $J = 5.70$ Hz), 3.31 (t, 2H, $J = 5.70$ Hz); ^{13}C NMR (100 MHz, DMSO-d_6) δ (ppm): 150.3, 145.9, 133.4, 130.5, 129.8, 118.3, 116.0, 113.6, 112.4, 109.5, 42.9, 42.8, 38.3; HRMS m/z: 370.0 [M + H]$^+$.

4.7.7. 3-((2-(p-Tolylamino)ethyl)amino)benzenesulfonamide (6n)

Brown solid. Yield = 42%, silica gel TLC R_f 0.50 (EtOAc/Hex 50% v/v); ^{1}H NMR (400 MHz, DMSO-d_6) δ (ppm): 7.27 (t, 1H, $J = 7.82$ Hz), 7.20 (s, 2H), 7.07 (s, 1H), 7.01 (s, 1H, $J = 7.13$ Hz), 6.94 (d, 2H, $J = 7.82$ Hz), 6.80 (d, 1H, $J = 6.90$ Hz), 6.55 (d, 2H, $J = 8.01$ Hz), 6.17 (s, 1H), 5.42 (s, 1H), 3.26 (s, 4H), 2.19 (s, 3H); ^{13}C NMR (100 MHz, DMSO-d_6) δ (ppm): 152.3, 148.4, 131.5, 129.8, 128.5, 120.1, 113.9, 112.5, 43.3, 42.7; HRMS m/z: 306.1 [M + H]$^+$.

4.7.8. 3-((2-((4-Chlorophenyl)amino)ethyl)amino)benzenesulfonamide (6o)

Black solid. M.p. 185–187 °C. Yield = 80%, silica gel TLC R_f 0.39 (EtOAc/Hex 50% v/v); ^{1}H NMR (400 MHz, DMSO-d_6) δ (ppm): 7.27 (t, 1H, $J = 8.02$ Hz), 7.20 (bs, 1H), 7.12 (d, 2H, $J = 8.82$ Hz), 7.06 (s, 1H), 7.00 (d, 1H, $J = 7.62$ Hz), 6.91 (s, 1H), 6.79 (d, 1H, $J = 8.02$ Hz), 6.63 (d, 2H, $J = 8.42$ Hz), 6.18 (s, 1H), 5.90 (s, 1H), 3.26 (s, 4H); ^{13}C NMR (100 MHz, DMSO-d_6) δ (ppm): 150.0, 148.6, 145.7, 130.4, 129.7, 120.2, 116.1, 114.5, 113.6, 109.4, 42.9, 31.5; HRMS m/z: 326.1 [M + H]$^+$.

4.8. General procedure for compounds 7a–j and 8k–o

To a stirring solution of the appropriate derivative **7a–j** or **8k–o** (0.15 mmol, 1 eq.) in dry THF (10 mL), a solution of triphosgene (22.8 mg, 0.08 mmol, 0.5 eq.) in dry THF (2.5 mL) was added dropwise at r.t. The resulting mixture was stirred at room temperature for 1 h under a nitrogen atmosphere., then dry TEA (21 µL, 0.154 mmol, 1 eq.) was added and the mixture was stirred at room temperature for 1 h under a nitrogen atmosphere. Then, the reaction was quenched with water and extracted with EtOAc three times. The combined organic layers were washed with brine, dried over anhydrous Na_2SO_4, filtered, and evaporated under vacuum. The reaction crudes were purified by silica gel flash column chromatography.

4.8.1. 4-(3-Isopropyl-2-oxoimidazolidin-1-yl)benzenesulfonamide (7a)

Brown solid. M.p. 243–245 °C. Yield = 52%, silica gel TLC R_f 0.30 (EtOAc/Hex 70% v/v); ^{1}H NMR (400 MHz, DMSO-d_6) δ (ppm): 7.74 (m, 4H), 7.21 (bs, 2H), 3.84 (t, 2H, $J = 8.44$ Hz), 3.46 (t, 2H, $J = 8.12$ Hz); ^{13}C NMR (100 MHz, DMSO-d_6) δ (ppm): 156.4, 144.0, 136.8, 126.9, 116.4, 43.7, 42.4, 36.3, 19.7; HRMS m/z: 284.1 [M + H]$^+$.

4.8.2. 4-(3-Butyl-2-oxoimidazolidin-1-yl)benzenesulfonamide (7b)

Brown solid. M.p. 274–276 °C. Yield = 38%, silica gel TLC R_f 0.1 (MeOH/DCM 10% v/v); ^{1}H NMR (400 MHz, DMSO-d_6) δ (ppm): 7.81 (m, 4H), 7.27 (s, 2H), 1.45 (m, 2H), 1.36 (m, 2H), 1.13 (t, 2H, $J = 7.16$ Hz), 0.92 (t, 3H, $J = 7.40$ Hz); ^{13}C NMR (100 MHz, DMSO-d_6) δ (ppm): 159.1, 146.7, 136.5, 129.4, 121.9, 49.5, 41.8, 29.5, 26.4, 19.7, 13.8; HRMS m/z: 298.1 [M + H]$^+$.

4.8.3. 4-(2-Oxo-3-phenylimidazolidin-1-yl)benzenesulfonamide (7c)

White solid. Yield = 63%, silica gel TLC R_f 0.31 (MeOH/DCM 5% v/v); ^{1}H NMR (400 MHz, DMSO-d_6) δ (ppm): 7.84 (s, 4H), 7.68 (s, 2H, J = 8.24 Hz), 7.43 (t, 2H, J = 7.76 Hz), 7.30 (s, 2H), 7.14 (t, 1H, J = 7.27 Hz), 4.06 (s, 4H); ^{13}C NMR (100 MHz, DMSO-d_6) δ (ppm): 155.3, 144.1, 140.9, 138.5, 129.8, 127.6, 123.9, 119.1, 118.1, 42.5; HRMS m/z: 318.1 [M + H]$^+$.

4.8.4. 4-(3-(2-Fluorophenyl)-2-oxoimidazolidin-1-yl)benzenesulfonamide (7d)

Brown solid. M.p. 221–223 °C. Yield = 73%, silica gel TLC R_f 0.45 (EtOAc/DCM 70% v/v); ^{1}H NMR (400 MHz, DMSO-d_6) δ (ppm): 7.81 (m, 4H), 7.58 (m, 1H), 7.31 (m, 2H), 7.21 (m, 2H), 4.05 (m, 2H), 3.95 (m, 2H); HRMS m/z: 336.1 [M + H]$^+$ in agreement with[34].

4.8.5. 4-(3-(2-Bromophenyl)-2-oxoimidazolidin-1-yl)benzenesulfonamide (7e)

Brown solid. M.p. 241–243 °C. Yield = 95%, silica gel TLC R_f 0.30 (MeOH/DCM 3% v/v); ^{1}H NMR (400 MHz, DMSO-d_6) δ (ppm): 7.83 (m, 5H), 7.60 (dd, 1H, J = 7.89 Hz, J = 6.44 Hz), 7.53 (t, 1H, J = 7.89 Hz), 7.37 (m, 1H), 7.29 (s, 2H), 4.12 (t, 2H, J = 8.42 Hz), 3.94 (t, 2H, J = 8.42 Hz); ^{13}C NMR (100 MHz, DMSO-d_6) δ (ppm): 155.5, 143.5, 138.4, 197.7, 133.7, 130.8, 130.1, 129.3, 127.0, 123.1, 117.0, 44.2, 42.9; HRMS m/z: 396.0 [M + H]$^+$.

4.8.6. 4-(2-Oxo-3-(p-tolyl)imidazolidin-1-yl)benzenesulfonamide (7f)

Brown solid. M.p. 279–281 °C. Yield = 27%, silica gel TLC R_f 0.32 (MeOH/DCM 5% v/v); ^{1}H NMR (400 MHz, DMSO-d_6) δ (ppm): 7.84 (s, 4H), 7.56 (d, 2H, J = 8.56 Hz), 7.29 (s, 2H), 7.23 (d, 2H, J = 8.56 Hz), 4.03 (s, 4H), 2.33 (s, 3H); HRMS m/z: 332.1 [M + H]$^+$ in agreement with[34].

4.8.7. 4-(3-(4-Chlorophenyl)-2-oxoimidazolidin-1-yl)benzenesulfonamide (7g)

Black solid. M.p. 267–269 °C. Yield = 35%, silica gel TLC R_f 0.55 (MeOH/DCM 3% v/v); ^{1}H NMR (400 MHz, DMSO-d_6) δ (ppm): 7.84 (s, 4H), 7.72 (d, 2H, J = 9.12 Hz), 7.48 (d, 2H, J = 9.12 Hz), 7.30 (s, 2H), 4.05 (s, 4H); ^{13}C NMR (100 MHz, DMSO-d_6) δ (ppm): 155.1, 143.8, 139.8, 138.6, 129.6, 127.6, 125.9, 120.5, 118.3, 42.4, 31.5; HRMS m/z: 352.0 [M + H]$^+$.

4.8.8. 4-(3-(4-Iodophenyl)-2-oxoimidazolidin-1-yl)benzenesulfonamide (7h)

Brown solid. M.p. 250–252 °C. Yield = 45%, silica gel TLC R_f 0.47 (EtOAc/Hex 60% v/v); ^{1}H NMR (400 MHz, DMSO-d_6) δ (ppm): 7.55 (d, 4H, J = 8.68 Hz), 6.97 (bs, 2H), 6.71 (d, 4H, J = 8.67 Hz), 3.75 (t, 2H, J = 6.19 Hz), 3.50 (t, 2H, J = 6.19 Hz); ^{13}C NMR (100 MHz, DMSO-d_6) δ (ppm): 154.5, 143.2, 139.2, 137.9, 129.0, 127.0, 119.9, 117.5, 114.4, 41.8, 30.9; HRMS m/z: 444.0 [M + H]$^+$.

4.8.9. 4-(3-(6-Methylpyridin-2-yl)-2-oxoimidazolidin-1-yl)benzenesulfonamide (7i)

Yellow solid. Yield = 34%, silica gel TLC R_f 0.40 (EtOAc/Hex 70% v/v); ^{1}H NMR (400 MHz, DMSO-d_6) δ (ppm): 8.05 (d, 2H, J = 8.27 Hz), 7.84 (s, 4H), 7.71 (t, 1H, J = 7.85 Hz), 7.28 (s, 2H), 4.14 (t, 2H, J = 8.63 Hz), 4.02 (t, 2H, J = 8.40 Hz); ^{13}C NMR (100 MHz, DMSO-d_6) δ (ppm): 155.7, 154.6, 152.3, 146.7, 138.5, 136.5, 129.4, 121.9, 119.0, 26.0, 23.9; HRMS m/z: 333.1 [M + H]$^+$.

4.8.10. 4-(3-Benzyl-2-oxoimidazolidin-1-yl)benzenesulfonamide (7j)

White solid. M.p. 244–246 °C. Yield = 65%, silica gel TLC R_f 0.38 (EtOAc/Hex 70% v/v); ^{1}H NMR (400 MHz, DMSO-d_6) δ (ppm): 7.78 (s, 4H), 7.39 (t, 2H, J = 7.31 Hz), 7.33 (d, 3H, J = 7.52 Hz), 7.22 (s, 2H), 4.44 (s, 2H), 3.88 (t, 2H, J = 8.42 Hz), 3.42 (t, 2H, J = 7.77 Hz); ^{13}C NMR (100 MHz, DMSO-d_6) δ (ppm): 157.8, 144.5, 138.0, 137.7, 129.7, 128.9, 128.4, 127.6, 117.2, 48.1, 42.9, 41.8; HRMS m/z: 332.1 [M + H]$^+$.

4.8.11. 3-(3-Butyl-2-oxoimidazolidin-1-yl)benzenesulfonamide (8k)

Brown solid. M.p. 177–179 °C. Yield = 37%, silica gel TLC R_f 0.40 (EtOAc/Hex 60% v/v); ^{1}H NMR (400 MHz, DMSO-d_6) δ (ppm): 8.18 (s, 1H), 7.71 (d, 1H, J = 8.26 Hz), 7.51 (t, 1H, J = 8.26 Hz), 7.46 (d, 1H, J = 7.80 Hz), 7.36 (s, 2H), 3.86 (t, 2H, J = 8.49 Hz), 3.52 (t, 2H, J = 8.20 Hz), 3.24 (t, 2H, J = 7.07 Hz), 1.53 (t, 2H, J = 7.23 Hz), 1.34 (m, 2H), 0.95 (t, 3H, J = 7.43 Hz); ^{13}C NMR (100 MHz, DMSO-d_6) δ (ppm): 157.9, 145.6, 142.2, 130.3, 120.4, 119.4, 114.7, 43.8, 43.0, 41.9, 29.9, 20.5. 14.7; HRMS m/z: 298.1 [M + H]$^+$.

4.8.12. 3-(2-Oxo-3-phenylimidazolidin-1-yl)benzenesulfonamide (8l)

Brown solid. M.p. 215–217 °C. Yield = 51%, silica gel TLC R_f 0.31 (MeOH/DCM 5% v/v); ^{1}H NMR (400 MHz, DMSO-d_6) δ (ppm): 8.26 (s, 1H), 7.79 (d, 1H, J = 7.79 Hz), 7.68 (d, 2H, J = 8.08 Hz), 7.58 (m, 2H), 7.42 (m, 4H), 7.13 (t, 1H, J = 7.27 Hz), 4.05 (s, 4H); ^{13}C NMR (100 MHz, DMSO-d_6) δ (ppm): 155.3, 145.7, 141.6, 140.9, 130.4, 129.8, 123.8, 121.4, 120.3, 118.9, 115.7, 42.5; HRMS m/z: 318.1 [M + H]$^+$.

4.8.13. 3-(3-(2-Bromophenyl)-2-oxoimidazolidin-1-yl)benzenesulfonamide (8m)

Brown solid. Yield = 68%, silica gel TLC R_f 0.57 (EtOAc/Hex 70% v/v); ^{1}H NMR (400 MHz, DMSO-d_6) δ (ppm): 8.22 (s, 1H), 7.77 (apt, 2H, J = 7.39 Hz), 7.53 (m, 4H), 7.38 (bs, 3H), 4.08 (apt, 2H, J = 5.54 Hz), 3.93 (apt, 2H, J = 5.54 Hz); ^{13}C NMR (100 MHz, DMSO-d_6) δ (ppm): 156.3, 145.7, 141.7, 139.0, 134.3, 131.3, 130.7, 130.5, 129.9, 123.7, 121.0, 120.2, 115.3, 44.9, 43.7; HRMS m/z: 395.9 [M + H]$^+$.

4.8.14. 3-(2-Oxo-3-(p-tolyl)imidazolidin-1-yl)benzenesulfonamide (8n)

Brown solid. M.p. 183–185 °C. Yield = 37%, silica gel TLC R_f 0.48 (EtOAc/Hex 50% v/v); ^{1}H NMR (400 MHz, DMSO-d_6) δ (ppm): 8.26 (s, 1H), 7.78 (d, 1H, J = 9.07 Hz), 7.57 (m, 4H), 7.42 (s, 2H), 7.22 (d, 2H, J = 8.00 Hz), 4.02 (s, 4H), 2.23 (s, 3H); ^{13}C NMR (100 MHz, DMSO-d_6) δ (ppm): 154.7, 145.1, 141.0, 137.9, 132.2, 129.8, 129.6, 120.6, 119.6, 118.4, 114.9, 41.9, 20.8; HRMS m/z: 332.1 [M + H]$^+$.

4.8.15. 3-(3-(4-Chlorophenyl)-2-oxoimidazolidin-1-yl)benzenesulfonamide (8o)

Black solid. M.p. 185–187 °C. Yield = 60%, silica gel TLC R_f 0.40 (EtOAc/Hex 70% v/v); ^{1}H NMR (400 MHz, DMSO-d_6) δ (ppm): 8.26 (s, 1H), 7.79 (d, 1H, J = 7.85 Hz), 7.72 (dd, 2H, J = 8.98 Hz, J = 6.54 Hz), 7.58 (m, 2H), 7.47 (dd, 2H, J = 9.07 Hz, J = 6.46 Hz), 7.42 (s, 2H), 4.05 (s, 4H); ^{13}C NMR (100 MHz, DMSO-d_6) δ (ppm): 154.6, 145.1, 140.8, 139.3, 129.9, 129.0, 126.9, 120.8, 119.9, 119.8, 115.1, 41.9; HRMS m/z: 352.0 [M + H]$^+$.

4.9. In vitro carbonic anhydrase inhibition assay

The CA-catalyzed CO_2 hydration activity was performed on an Applied Photophysics stopped-flow instrument using phenol red,

at a concentration of 0.2 mM, as a pH indicator with 20 mM HEPES (pH 7.5) as the buffer, 20 mM Na_2SO_4, and following the initial rates of the CA-catalyzed CO_2 hydration reaction for a period of 10–100 s and working at the maximum absorbance of 557 nm. The CO_2 concentrations ranged from 1.7 to 17 mM. For each inhibitor, six traces of the initial 5−10% of the reaction have been used to determine the initial velocity. The uncatalyzed reaction rates were determined in the same manner and subtracted from the total observed rates. Stock solutions of inhibitor (0.1 mM) were prepared in distilled water, and dilutions up to 0.01 nM were prepared. Solutions containing inhibitor and enzyme were preincubated for 15 min at room temperature before assay to allow the formation of the E−I complex. The inhibition constants were obtained as non-linear least-squares protocols using PRISM 3 and are the mean from at least three different measurements. All CAs were recombinant ones and were obtained in house[42,43].

4.10. Cell culture and reagents

Human U87MG (ATCC HTB-14), U251 (Merck U-251 MG), T98G (ATCC CRL-1690) cells and human breast cancer MDA-MB-468 cells (ATCC HTB-132) and MCF-7 (ATCC HTB-2) were grown in DMEM supplemented with 10% FCS. Human pancreatic cancer CF-PAC-1 (ATCC CRL-1918) and PANC-1 (ATCC CRL-1469) cells were grown in RPMI 1640 supplemented with 10% FCS. Cells were kept at the low passage, returning to original frozen stocks every 3–4 months. Hypoxic culture conditions were realised in the presence of 1% O_2 and 5% CO_2.

4.11. Quantitative PCR

Cells were cultured at 37 °C with 1% O_2 and 5% CO_2 for 24 h. Total RNA was isolated using TRIzol Reagent (Invitrogen) according to the manufacturer's instructions. Two μg of total RNA were retro-transcribed with MMLV reverse transcriptase (Invitrogen) using random primers. cDNA was analysed by quantitative real-time polymerase chain reaction (qPCR) analysis. β-Actin was used as a housekeeping gene for normalisation. Primers used: Hs-CAIX forward: 5′-CTTTGAATGGGCGAGTGATT-3′, reverse: 5′-TTCTGTG CTGCCTTCTCATCT-3′; Hs-B-actin forward: 5′-CACACAGGGGAG GTGATAGC-3′, reverse: 5′-GACCAAAAGCCTTCATACATCTCA-3′.

4.12. Cell proliferation assay

The different cellular lines were seeded in 48-well plates and treated in 1% FBS with increasing concentrations of compounds **7a**, **7d**, and **8m** or **SLC-0111**. After 72 h of incubation at 37 °C with 1% O_2, 5% CO_2, and 94% N_2, cells were trypsinized and cell counting was performed with the MACSQuant® Analyser (Miltenyi Biotec)[44].

Author contributions

The manuscript was written with the contributions of all authors. All authors have approved the final version of the manuscript.

Disclosure statement

C.T. Supuran is Editor-in-Chief of the Journal of Enzyme Inhibition and Medicinal Chemistry. He was not involved in the assessment, peer review, or decision-making process of this paper. The authors have no relevant affiliations or financial involvement with any organisation or entity with a financial interest in or financial conflict with the subject matter or materials discussed in the manuscript. F. Carta and C.T. Supuran declare a conflict of interest, being co-discoverers of **SLC-0111**. This includes employment, consultancies, honoraria, stock ownership or options, expert testimony, grants or patents received or pending, or royalties.

ORCID

Simone Carradori   http://orcid.org/0000-0002-8698-9440
Claudiu T. Supuran   http://orcid.org/0000-0003-4262-0323

References

1. Supuran CT. Structure and function of carbonic anhydrases. Biochem J 2016;473:2023–32.
2. Supuran CT. Carbonic anhydrases: novel therapeutic applications for inhibitors and activators. Nat Rev Drug Discov 2008;7:168–81.
3. McKenna R, Supuran CT. Carbonic anhydrase inhibitors drug design. Subcell Biochem 2014;75:291–323.
4. Alterio V, Fiore AD, D'Ambrosio K, et al. Multiple binding modes of inhibitors to carbonic anhydrases: how to design specific drugs targeting 15 different isoforms? Chem Rev 2012;112:4421–68.
5. Akman M, Belisario DC, Salaroglio IC, et al. Hypoxia, endoplasmic reticulum stress and chemoresistance: dangerous liaisons. J Exp Clin Cancer Res 2021;40:28.
6. Supuran CT. Experimental carbonic anhydrase inhibitors for the treatment of hypoxic tumors. J Exp Pharmacol 2020;12:603–17.
7. Supuran CT, Alterio V, Di Fiore A, et al. Inhibition of carbonic anhydrase IX targets primary tumors, metastases, and cancer stem cells: three for the price of one. Med Res Rev 2018;38: 1799–836.
8. Güttler A, Theuerkorn K, Riemann A, et al. Cellular and radiobiological effects of carbonic anhydrase IX in human breast cancer cells. Oncol Rep 2019;41:2585–94.
9. Koyuncu I, Gonel A, Durgun M, et al. Assessment of the anti-proliferative and apoptotic roles of sulfonamide carbonic anhydrase IX inhibitors in HeLa cancer cell line. J Enzyme Inhib Med Chem 2019;34:75–86.
10. Hsin MC, Hsieh YH, Hsiao YH, et al. Carbonic anhydrase IX promotes human cervical cancer cell motility by regulating PFKFB4 expression. Cancers 2021;13:1174.
11. Chan N, Koritzinsky M, Zhao H, et al. Chronic hypoxia decreases synthesis of homologous recombination proteins to offset chemoresistance and radioresistance. Cancer Res 2008;68:605–14.
12. Kondo A, Safaei R, Mishima M, et al. Hypoxia-induced enrichment and mutagenesis of cells that have lost DNA mismatch repair. Cancer Res 2001;61:7603–7.

13. Kato Y, Yashiro M, Fuyuhiro Y, et al. Effects of acute and chronic hypoxia on the radiosensitivity of gastric and esophageal cancer cells. Anticancer Res 2011;31:3369–75.

14. Chaplin DJ, Durand RE, Olive PL. Acute hypoxia in tumors: implications for modifiers of radiation effects. Int J Radiat Oncol Biol Phys 1986;12:1279–82.

15. Rofstad EK, Gaustad JV, Egeland TA, et al. Tumors exposed to acute cyclic hypoxic stress show enhanced angiogenesis, perfusion and metastatic dissemination. Int J Cancer 2010;127: 1535–46.

16. Minassian LM, Cotechini T, Huitema E, Graham CH. Hypoxia-induced resistance to chemotherapy in cancer. Adv Exp Med Biol 2019;1136:123–39.

17. Kuchuk O, Tuccitto A, Citterio D, et al. pH regulators to target the tumor immune microenvironment in human hepato-cellular carcinoma. Oncoimmunology 2018;7:e1445452.

18. Ward C, Langdon SP, Mullen P, et al. New strategies for targeting the hypoxic tumour microenvironment in breast cancer. Cancer Treat Rev 2013;39:171–9.

19. Tawfik HO, Petreni A, Supuran CT, El-Hamamsy MH. Discovery of new carbonic anhydrase IX inhibitors as anti-cancer agents by toning the hydrophobic and hydrophilic rims of the active site to encounter the dual-tail approach. Eur J Med Chem 2022;232:114190.

20. Koyuncu I, Temiz E, Durgun M, et al. Intracellular pH-mediated induction of apoptosis in HeLa cells by a sulfonamide carbonic anhydrase inhibitor. Int J Biol Macromol 2022;201:37–46.

21. Mussi S, Rezzola S, Chiodelli P, et al. Antiproliferative effects of sulphonamide carbonic anhydrase inhibitors C18, SLC-0111 and acetazolamide on bladder, glioblastoma and pancreatic cancer cell lines. J Enzyme Inhib Med Chem 2022;37:280–6.

22. (a) Lau J, Zhang Z, Jenni S, et al. PET imaging of carbonic anhydrase IX expression of HT-29 tumor xenograft mice with (68)Ga-labeled benzenesulfonamides. Mol Pharm 2016;13: 1137–46.(b) Mishra CB, Mongre RK, Prakash A, et al. Anti-breast cancer action of carbonic anhydrase IX inhibitor 4-[4-(4-Benzo[1,3]dioxol-5-ylmethyl-piperazin-1-yl)-benzylidene-hydrazi-nocarbonyl]-benzenesulfonamide (BSM-0004): in vitro and in vivo studies. J Enzyme Inhib Med Chem 2021;36:954–63.

23. Chafe SC, Vizeacoumar FS, Venkateswaran G, et al. Genome-wide synthetic lethal screen unveils novel CAIX-NFS1/xCT axis as a targetable vulnerability in hypoxic solid tumors. Sci Adv 2021;7:eabj0364.

24. McDonald PC, Chia S, Bedard PL, et al. A phase 1 study of SLC-0111, a novel inhibitor of carbonic anhydrase IX, in patients with advanced solid tumors. Am J Clin Oncol 2020; 43:484–90.

25. Andreucci E, Ruzzolini J, Peppicelli S, et al. The carbonic anhydrase IX inhibitor SLC-0111 sensitises cancer cells to conventional chemotherapy. J Enzyme Inhib Med Chem 2019;34:117–23.

26. Hedlund EE, McDonald PC, Nemirovsky O, et al. Harnessing induced essentiality: targeting carbonic anhydrase IX and angiogenesis reduces lung metastasis of triple negative breast cancer xenografts. Cancers 2019;11:1002.

27. Boyd NH, Walker K, Fried J, et al. Addition of carbonic anhydrase 9 inhibitor SLC-0111 to temozolomide treatment delays glioblastoma growth in vivo. JCI Insight 2017;2: e92928.

28. McDonald PC, Chafe SC, Brown WS, et al. Regulation of pH by carbonic anhydrase 9 mediates survival of pancreatic cancer cells with activated KRAS in response to hypoxia. Gastroenterology 2019;157:823–37.

29. Pacchiano F, Carta F, McDonald PC, et al. Ureido-substituted benzenesulfonamides potently inhibit carbonic anhydrase IX and show antimetastatic activity in a model of breast cancer metastasis. J Med Chem 2011;54:1896–902.

30. Mboge MY, Mahon BP, Lamas N, et al. Structure activity study of carbonic anhydrase IX: selective inhibition with ureido-substituted benzenesulfonamides. Eur J Med Chem 2017;132:184–91.

31. Akdemir ÖG, Yazıcı KD, Vullo D, et al. New pyridinium salt derivatives of 2-(hydrazinocarbonyl)-3-phenyl-1H-indole-5-sulfonamide as selective inhibitors of tumour-related human carbonic anhydrase isoforms IX and XII. Anticancer Agents Med Chem 2022;22:2637–2646.

32. Bozdag M, Carta F, Ceruso M, et al. Discovery of 4-hydroxy-3-(3-(phenylureido)benzenesulfonamides as SLC-0111 analogues for the treatment of hypoxic tumors overexpressing carbonic anhydrase IX. J Med Chem 2018;61:6328–38.

33. Mboge MY, Combs J, Singh S, et al. Inhibition of carbonic anhydrase using SLC-149: support for a noncatalytic function of CAIX in breast cancer. J Med Chem 2021;64:1713–24.

34. Zhang Z. Aryl sulfonamide compounds as carbonic anhydrase inhibitors and their therapeutic use. 2017. WO 2017/004543 A1.

35. Supuran CT, Scozzafava A, Jurca BC, Ilies MA. Carbonic anhydrase inhibitors. Part 49. Synthesis of substituted ureido- and thioureido derivatives of aromatic/heterocyclic sulfonamides with increased affinities for isozyme I. Eur J Med Chem 1998;33:83–93.

36. Kalifah RG. The carbon dioxide hydration activity of carbonic anhydrase I. Stop-flow kinetic studies on the native human isoenzymes b and c. J Biol Chem 1971;246:2561–73.

37. Supuran CT. Carbonic anhydrase inhibitors: an update on experimental agents for the treatment and imaging of hypoxic tumors. Expert Opin Investig Drugs 2021;30:1197–208.

38. Sarnella A, Ferrara Y, Auletta L, et al. Inhibition of carbonic anhydrases IX/XII by SLC-0111 boosts cisplatin effects in hampering head and neck squamous carcinoma cell growth and invasion. J Exp Clin Cancer Res 2022;41:122.

39. Daina A, Michielin O, Zoete V. SwissADME: a free web tool to evaluate pharmacokinetics, drug-likeness and medicinal chemistry friendliness of small molecules. Sci Rep 2017;7: 42717.

40. Lagorce D, Bouslama L, Becot J, et al. FAF-Drugs4: free ADME-tox filtering computations for chemical biology and early stages drug discovery. Bioinformatics 2017;33:3658–60.

41. Baell JB, Holloway GA. New substructure filters for removal of Pan assay interference compounds (PAINS) from screening libraries and for their exclusion in bioassays. J Med Chem 2010;53:2719–40.

42. D'Ambrosio K, Carradori S, Cesa S, et al. Catechols: a new class of carbonic anhydrase inhibitors. Chem Commun 2020; 56:13033–6.

43. Carradori S, De Monte C, D'Ascenzio M, et al. Salen and tetrahydrosalen derivatives act as effective inhibitors of the tumor-associated carbonic anhydrase XII–a new scaffold for designing isoform-selective inhibitors. Bioorg Med Chem Lett 2013;23:6759–63.

44. Giacomini A, Taranto S, Rezzola S, et al. Inhibition of the FGF/FGFR system induces apoptosis in lung cancer cells via c-Myc downregulation and oxidative stress. Int J Mol Sci 2020;21:9376.